

# vinculin (7F9): sc-73614

## BACKGROUND

Focal adhesions are identified as areas within the plasma membrane of tissue culture cells that adhere tightly to the underlying substrate. *In vivo*, these regions are involved in the adhesion of cells to the extracellular matrix. Paxillin and vinculin are cytoskeletal, focal adhesion proteins that are components of a protein complex which links the Actin network to the plasma membrane. Vinculin binding sites have been identified on other cytoskeletal proteins, including Talin and  $\alpha$ -actinin. In addition, vinculin, Talin and  $\alpha$ -actinin each contain Actin binding sites. Expression of vinculin and Talin have been shown to be affected by the level of Actin expression.  $\alpha$ -actinin has been shown to link Actin to integrins in the plasma membrane through interactions with the vinculin and Talin complex or by a direct interaction with integrin.

## CHROMOSOMAL LOCATION

Genetic locus: VCL (human) mapping to 10q22.2; Vcl (mouse) mapping to 14 A3.

## SOURCE

vinculin (7F9) is a mouse monoclonal antibody raised against vinculin of human origin.

## PRODUCT

Each vial contains 200  $\mu$ g IgG<sub>1</sub> kappa light chain in 1.0 ml of PBS with < 0.1% sodium azide and 0.1% gelatin.

vinculin (7F9) is available conjugated to agarose (sc-73614 AC), 500  $\mu$ g/0.25 ml agarose in 1 ml, for IP; to HRP (sc-73614 HRP), 200  $\mu$ g/ml, for WB, IHC(P) and ELISA; to either phycoerythrin (sc-73614 PE), fluorescein (sc-73614 FITC), Alexa Fluor® 488 (sc-73614 AF488), Alexa Fluor® 546 (sc-73614 AF546), Alexa Fluor® 594 (sc-73614 AF594) or Alexa Fluor® 647 (sc-73614 AF647), 200  $\mu$ g/ml, for WB (RGB), IF, IHC(P) and FCM; and to either Alexa Fluor® 680 (sc-73614 AF680) or Alexa Fluor® 790 (sc-73614 AF790), 200  $\mu$ g/ml, for Near-Infrared (NIR) WB, IF and FCM.

Alexa Fluor® is a trademark of Molecular Probes, Inc., Oregon, USA

## APPLICATIONS

vinculin (7F9) is recommended for detection of vinculin of mouse, rat, human and avian origin by Western Blotting (starting dilution 1:200, dilution range 1:100-1:1000), immunoprecipitation [1-2  $\mu$ g per 100-500  $\mu$ g of total protein (1 ml of cell lysate)], immunofluorescence (starting dilution 1:50, dilution range 1:50-1:500) and immunohistochemistry (including paraffin-embedded sections) (starting dilution 1:50, dilution range 1:50-1:500).

Suitable for use as control antibody for vinculin siRNA (h): sc-29524, vinculin siRNA (m): sc-36819, vinculin siRNA (r): sc-270542, vinculin shRNA Plasmid (h): sc-29524-SH, vinculin shRNA Plasmid (m): sc-36819-SH, vinculin shRNA Plasmid (r): sc-270542-SH, vinculin shRNA (h) Lentiviral Particles: sc-29524-V, vinculin shRNA (m) Lentiviral Particles: sc-36819-V and vinculin shRNA (r) Lentiviral Particles: sc-270542-V.

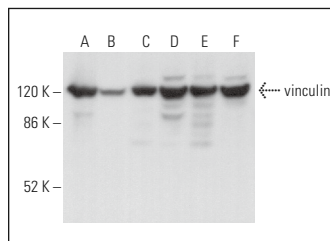
Molecular Weight of vinculin: 117 kDa.

Positive Controls: HeLa whole cell lysate: sc-2200, HUV-EC-C whole cell lysate: sc-364180 or K-562 whole cell lysate: sc-2203.

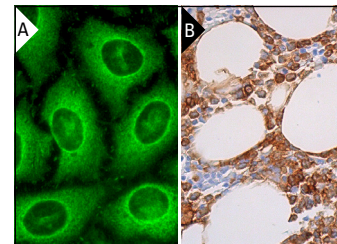
## STORAGE

Store at 4° C, **\*\*DO NOT FREEZE\*\***. Stable for one year from the date of shipment. Non-hazardous. No MSDS required.

## DATA



vinculin (7F9): sc-73614. Western blot analysis of vinculin expression in HeLa (A), K-562 (B), PC-3 (C), HUV-EC-C (D), ECV304 (E) and 3T3-L1 (F) whole cell lysates. Detection reagent used: m-IgGκ: BP-HRP: sc-516102.



vinculin (7F9): sc-73614. Immunofluorescence staining of methanol-fixed HeLa cells showing cytoplasmic localization (A). Immunoperoxidase staining of formalin fixed, paraffin-embedded human bone marrow tissue showing cytoplasmic staining of hematopoietic cells (B).

## SELECT PRODUCT CITATIONS

- Korshunov, A., et al. 2000. Immunohistochemical markers for intracranial ependymoma recurrence. An analysis of 88 cases. *J. Neurol. Sci.* 177: 72-82.
- Hoppe-Seyler, K., et al. 2017. Induction of dormancy in hypoxic human papillomavirus-positive cancer cells. *Proc. Natl. Acad. Sci. USA* 114: E990-E998.
- Avolio, R., et al. 2018. Protein Syndesmos is a novel RNA-binding protein that regulates primary cilia formation. *Nucleic Acids Res.* 46: 12067-12086.
- Schnack, L., et al. 2019. Mechanisms of trained innate immunity in oxLDL primed human coronary smooth muscle cells. *Front. Immunol.* 10: 13.
- Ballabio, C., et al. 2020. Modeling medulloblastoma *in vivo* and with human cerebellar organoids. *Nat. Commun.* 11: 583.
- Hollenbach, M., et al. 2021. Pitfalls in AR42J-model of cerulein-induced acute pancreatitis. *PLoS ONE* 16: e0242706.
- Yockteng-Melgar, J., et al. 2022. G<sub>1</sub>/S cell cycle induction by Epstein-Barr virus BORF2 is mediated by P53 and APOBEC3B. *J. Virol.* 96: e0066022.
- Bohn, P., et al. 2023. A dsRNA-binding mutant reveals only a minor role of exonuclease activity in interferon antagonism by the arenavirus nucleoprotein. *PLoS Pathog.* 19: e1011049.
- Russo, M., et al. 2024. Acetyl-CoA production by mediator-bound 2-ketoacid dehydrogenases boosts de novo histone acetylation and is regulated by nitric oxide. *Mol. Cell* 84: 967-980.e10.
- Marañón, P., et al. 2025. BMP6 participates in the molecular mechanisms involved in APAP hepatotoxicity. *Arch. Toxicol.* 99: 1187-1202.

## RESEARCH USE

For research use only, not for use in diagnostic procedures.